OESTERREICHISCHE NATIONALBANK
EUROSYSTEM

ChaMP

Working Paper 276

Are there asymmetries in euro area monetary policy?

Michael Pfarrhofer, Anna Stelzer

OeNB Working Paper Series
40 pages

Are there asymmetries in euro area monetary policy?

This paper examines asymmetries and nonlinearities in the effects of monetary policy on the aggregate euro area. Using a non-linear mixed-frequency model that explicitly models lending via banks, the authors identify significant asymmetries. Monetary tightening has clear and persistent effects on credit, output and inflation, while easing has weak or insignificant effects. These results change little over the business cycle or at the effective lower bound.

Authors

Michael Pfarrhofer
Vienna University of Economics and Business, Department of Economics, michael.pfarrhofer@wu.ac.at

Anna Stelzer
Oesterreichische Nationalbank, Monetary Policy, anna.stelzer@oenb.at

JEL classification
C32, E32, E52

Keywords
Nonlinear structural inference, mixed frequency data, Bayesian nonparametrics, credit channel

No assumptions of form of nonlinearities

We use a flexible nonlinear empirical model to study asymmetries in monetary policy transmission in the euro area. Different to previous studies, we do not assume a specific functional form but instead let the model and the data speak on the presence of nonlinearities.

Monetary tightening is more powerful

The credit, bank lending, and borrower balance sheet all display asymmetries. Tightening has restrictive effects, while easing is not amplified in a comparable way by bank lending. These asymmetries are transmitted to output and inflation, which show strong and persistent responses to tightening.

Limited economic state-dependence

There is little variation of monetary policy effects over the business cycle and distinct periods such as the effective lower bound, suggesting asymmetries are not primarily driven by economic state.

Challenges for Monetary Policy Transmission in a Changing World Network (ChaMP)

This paper contains research conducted within the network "Challenges for Monetary Policy Transmission in a Changing World Network" (ChaMP). It consists of economists from the European Central Bank (ECB) and the national central banks (NCBs) of the European System of Central Banks (ESCB).

ChaMP is coordinated by a team chaired by Philipp Hartmann (ECB), and consisting of Diana Bonfim (Banco de Portugal), Margherita Bottero (Banca d'Italia), Emmanuel Dhyne (Nationale Bank van België/Banque Nationale de Belgique) and Maria T. Valderrama (Oesterreichische Nationalbank), who are supported by Melina Papoutsi and Gonzalo Paz-Pardo (both ECB), 7 central bank advisers and 8 academic consultants.

ChaMP seeks to revisit our knowledge of monetary transmission channels in the euro area in the context of unprecedented shocks, multiple ongoing structural changes and the extension of the monetary policy toolkit over the last decade and a half as well as the recent steep inflation wave and its reversal. More information is provided on its website.

Are there asymmetries in euro area monetary policy?

Michael PFARRHOFER
WU Vienna

Anna STELZER
Oesterreichische Nationalbank

We assess asymmetries, nonlinearities and state dependencies in dynamic responses of the euro area to monetary policy shocks. The dataset includes macroeconomic, financial, and survey-based variables measuring credit conditions and bank lending transmission channels. These data are observed at different frequencies. We propose a multivariate nonparametric mixed-frequency model, and discuss how to compute dynamic causal effects in a nonlinear context. The results suggest limited effects of expansionary policy shocks whereas contractionary shocks yield responses in line with theory. There is little variation over the business cycle and in distinct periods such as at the effective lower bound.

JEL: C32, E32, E52

Keywords: nonlinear structural inference, mixed frequency data, Bayesian nonparametrics, credit channel

Contact: Anna Stelzer (anna.stelzer@oenb.at), Monetary Policy Section, Oesterreichische Nationalbank (OeNB). *Address*: Otto-Wagner-Platz 3, 1090 Vienna. This research is part of the ESCB's Challenges for Monetary Policy Transmission in a Changing World (ChaMP) Research Network. We would like to thank participants of the 7th ChaMP WS1 workshop, the VGSE Research Seminar in Macroeconomics and an internal OeNB research seminar for useful comments and suggestions. The views expressed in this paper are those of the authors and do not necessarily reflect the views of the Oesterreichische Nationalbank or the Eurosystem.

NON-TECHNICAL SUMMARY

We investigate whether monetary policy transmits to the real economy proportionally (relative to the magnitude and direction of the policy action), and whether any effects remain constant over time. We study these questions using a set of economic, financial, and bank lending indicators, including variables from the Bank Lending Survey (BLS), providing information on how banks adjust credit standard. Methodologically, we develop a machine learning model that can flexibly capture complex relationships between many monthly and quarterly time series. This model is used to estimate how monetary policy propagates and affects the economy up to a horizon of two years. To be able to interpret our estimates causally, we rely on external high-frequency data which captures the non-systematic, surprise component of monetary policy. The corresponding indicator is a monetary policy shock, which enters our model as an exogenous and observed variable.

A monetary tightening is systematically more powerful than a monetary easing. Contractionary monetary policy produces significant and persistent responses. In contrast, expansionary policy yields muted or statistically insignificant effects. This asymmetry is also pronounced in bank-based transmission channels. Conversely, easing does not generate a comparable relaxation in credit conditions. The only consistent exception is credit demand, which shows a positive response to easing, though still smaller than the effects of tightening. We also investigate whether these asymmetries depend on economic conditions. Specifically, we compare responses during recessions and expansions and during periods at the effective lower bound (ELB). We find limited evidence of state dependence. This suggests that the asymmetric nature of policy transmission is rooted not in the business cycle or interest rate environment, but in more structural features of how banks and borrowers respond to monetary policy.

1. INTRODUCTION

Understanding how monetary policy transmits to the real economy is central to effective policy making. In the euro area (EA), where bank lending dominates corporate and household finance, bank-based transmission channels are particularly important (see, for instance, Lane, 2023). In this paper, we investigate whether monetary policy in the EA has asymmetric or nonlinear effects along the time dimension, particularly through bank-based transmission channels, using a flexible nonparametric framework.[1]

Bank-based transmission can be characterized by several different theoretical channels. These channels build on the view that banks are well suited for solving asymmetric information problems in the financial system in their role as financial intermediaries. Bernanke and Gertler (1995) define the credit channel based on the observation that monetary policy not only affects the general level of interest rates, but also the size of the external finance premium. This is because frictions in credit markets, such as imperfect information, can worsen during periods of tighter monetary policy, therefore increasing the wedge between the cost of funds raised externally and the opportunity cost of internal funding (i.e., the external finance premium). This mechanism between monetary policy and the external finance premium can amplify other transmission channels.

Bernanke and Gertler (1995) discuss two further sub-channels of the credit channel, the balance sheet and the bank lending channel. The balance sheet channel focuses on how monetary policy impacts the financial position of borrowers. Tighter monetary policy can deteriorate borrowers' balance sheets by reducing asset values and increasing liabilities, which makes it more difficult for the borrowers to obtain external financing. This, in turn, also adversely affects their spending and investment decisions. The bank lending channel on the other hand focuses on the role of banks in the transmission of

[1] We use the terms asymmetry and nonlinearity to refer to differences in the magnitude or direction of responses to positive versus negative policy shocks, to deviations from proportionality of responses to different shock sizes, and to differences over time due to state dependencies and distinct initial conditions when a shock materializes.

monetary policy. Tight monetary policy reduces banks' reserves and thus their ability to lend. When banks cut back on lending, borrowers who rely on bank loans face higher financing costs or reduced access to credit, which in turn affects their spending and investment. However, the strength and speed of these effects may not be uniform across different monetary policy stances.

Earlier empirical studies investigating the strength and relevance of the credit channel mostly focused on heterogeneous transmission of monetary policy due to differences in bank characteristics or across different countries. That is, these studies emphasized how differences in institutional banking settings like competition and individual bank characteristics such as liquidity or capital constraints, or differences related to local housing or labor markets can cause heterogeneous cross-country transmission of monetary policy (Peek *et al.*, 1995; Favero *et al.*, 1999; Boivin *et al.*, 2008; Barigozzi *et al.*, 2014; Corsetti *et al.*, 2021). Our paper builds on another related strand of the literature, that focuses on asymmetries and nonlinearities in monetary policy effects along a time dimension. Ciccarelli *et al.* (2013) find time-variation in bank-based monetary policy transmission and Dahlhaus (2017) finds that expansionary conventional monetary policy during times of high financial stress has stronger and more persistent effects on the economy than during normal times, differences due to nonlinearities in the balance sheet and bank lending channel. Similarly, Conti *et al.* (2024) find that banks' risk perception can have a material impact on monetary policy transmission to credit to non-financial corporations, reinforcing a monetary tightening.

Exploring nonlinearities, state-dependence or asymmetries in the effects of monetary policy is not new to the literature (see Weise, 1999; Primiceri, 2005; Sims and Zha, 2006; Tenreyro and Thwaites, 2016; Barnichon and Matthes, 2018; Hauzenberger *et al.*, 2021; Gargiulo *et al.*, 2025; Clark *et al.*, 2025, among many others). Most of this work finds that contractionary monetary policy is more potent than expansionary policy — as summarized in the "pushing on a string" metaphor (e.g., Tenreyro and Thwaites, 2016; Angrist *et al.*, 2018). However, structural breaks (for example, the period at the effective lower bound of nominal interest rates; huge variance shocks such as the COVID pandemic), or the shift from a prolonged time of below-average inflation to a high-inflation period poses many new challenges and questions for both researchers policy makers. The transmission of monetary policy in the face of related changes to the real economy and the financial system remains a relevant topic of research.

Much of the existing literature still relies on linear models that assume symmetric transmission, or impose certain structures of nonlinearity by design of the econometric model. Despite considerable research efforts, much about the nature, magnitude and implications of monetary policy shocks remains unknown or depends on explicit or implicit assumptions. Given the relative importance of bank based financing in the EA, we investigate possible nonlinearities in the transmission of monetary policy via banks. And, our nonparametric econometric approach is designed such that it can capture diverse types of nonlinearities and asymmetries subject to only comparatively weak assumptions about any explicit functional forms.

We use information on bank-based transmission channels as captured by data of the Bank Lending Survey (BLS). The BLS is a quarterly survey by the Eurosystem, which reports bank lending conditions in the EA since 2003. Besides addressing the important fact that EA household and corporate finance is predominantly bank-based, using these data is advantageous because they reflect monetary policy actions also when the policy rate is constrained by the effective lower bound. Inspired by Ciccarelli *et al.* (2013), we summarize the information contained in the survey into common factors to characterize the broad credit channel, the bank lending channel and the borrower balance sheet channel. Since BLS data is only available every three months, we choose a mixed-frequency (MF) model, which allows us to combine monthly and quarterly data.

Using a fully specified model for estimation (i.e., an iterative dynamic framework as opposed to a projection based approach) eases jointly modeling time series of mixed frequencies. This is because no information is lost by temporal aggregation to a common lowest frequency, and only comparatively weak assumptions have to be made when interpolating variables from a lower to a higher frequency, in a model-consistent way (compared with other interpolation schemes). To measure asymmetric effects of monetary policy shocks, we move beyond linear MF-VARs — one of the workhorse models in the MF context (see, e.g., Foroni and Marcellino, 2014; Schorfheide and Song, 2015) — which are limited to capturing symmetric and history-independent effects. Instead we use a nonparametric version estimated with Bayesian Additive Regression Trees (BART), as in Huber *et al.* (2023); Marcellino and Pfarrhofer (2025).

Our framework abstracts from identification in the sense that we treat the monetary policy shocks as observed and exogenous. In this context, we rely on the shock estimated by Jarociński and Karadi (2020), which they obtain with a combination of high-frequency identification and sign restrictions. A key advantage of our mixed-frequency approach is that there is no need to aggregate these shocks to the lowest common frequency and thereby "average out" important within-quarter variation, or introduce biases due to the aggregation scheme (see also Ghysels, 2016).

Our results indicate that contractionary monetary policy has strong and significant effects, while expansionary policy tends to produce muted or insignificant responses. An analysis of the impact responses of variables reveals that for static responses, both sign and size asymmetries are present in responses to monetary policy. Turning to dynamic responses, asymmetric reactions with regard to the sign of the monetary policy shock appears to be the main driver of dynamic nonlinearities. Credit channels, including bank lending and borrower balance sheet effects show clear asymmetries, especially with respect to the sign of a monetary policy shock. Tightening leads to a contraction in the credit channel, especially under large shocks. Monetary easing, however, has limited impact, even during recessions and away from the effective lower bound (ELB). Macroeconomic variables like output and inflation also exhibit stronger reactions to monetary tightening than easing. Inflation in particular shows nonlinear responses, with larger contractionary shocks having disproportionally smaller effects, while larger expansionary effects have a disproportionally larger impact on inflation.

The remainder of the paper is structured as follows. Section 2 provides further details about our econometric modeling framework. Section 3 discusses our model specifications and empirical findings. We conclude in section 4.

2. ECONOMETRIC FRAMEWORK

Throughout this paper we have a month-to-quarter frequency mismatch; the higher (monthly) frequency is indicated with $\mathtt{h}$ while the lower (quarterly) frequency is marked with $\mathtt{l}$.

On the quarterly frequency, we have measurements for $n_{\mathtt{l}}$ variables $\boldsymbol{y}^{*}_{\mathtt{l},t}$ each third month. This vector will contain, for instance, real GDP and the survey-based measures that we use to assess monetary transmission channels. By contrast, we observe $n_{\mathtt{h}}$ variables stacked in $\boldsymbol{y}_{\mathtt{h},t}$ each month. These include indicators of financial and economic activity that are measured more frequently, such as interest rates, unemployment or prices. We model an underlying latent monthly process $\boldsymbol{y}_{\mathtt{l},t}$ that is linked to the observed quarterly variables $\boldsymbol{y}^{*}_{\mathtt{l},t}$ with a set of measurement equations within a state space framework.

2.1. A general nonlinear mixed-frequency model

Let $\boldsymbol{y}_t = (\boldsymbol{y}'_{\mathtt{l},t}, \boldsymbol{y}'_{\mathtt{h},t})'$ be the $n \times 1$-vector of latent and observed monthly macroeconomic and financial variables (i.e., $n = n_{\mathtt{h}} + n_{\mathtt{l}}$). We assume that m independent, exogenous and unpredictable structural shocks, $\boldsymbol{\varepsilon}_t = (\varepsilon_{1t}, \ldots, \varepsilon_{mt})'$, are observed on a monthly frequency. That is, our framework assumes that direct measures or good proxies for any shock of interest are available. In our model specification, the shock of interest is the monetary policy shock, and $m = 1$. There is a long tradition of compiling series directly reflecting monetary policy shocks (e.g., Romer and Romer, 2004), so we treat this shock as data that is observed.

We use the following multivariate process as our state equation:

$$\boldsymbol{y}_t = \boldsymbol{F}(\boldsymbol{z}_t, \boldsymbol{\varepsilon}_t) + \boldsymbol{u}_t, \quad \boldsymbol{u}_t \sim \mathcal{N}(\boldsymbol{0}_n, \boldsymbol{\Sigma}_t), \tag{1}$$

where $\boldsymbol{z}_t = (\boldsymbol{y}'_{t-1}, \ldots, \boldsymbol{y}'_{t-p})'$. We define $\boldsymbol{x}_t = (\boldsymbol{z}'_t, \boldsymbol{\varepsilon}'_t)'$ and assume equation-specific functions $\boldsymbol{F}(\boldsymbol{z}_t, \boldsymbol{\varepsilon}_t) = \boldsymbol{F}(\boldsymbol{x}_t) = (f_1(\boldsymbol{x}_t), \ldots, f_n(\boldsymbol{x}_t))'$. The functional form is estimated from the data. We assume the covariance matrix to vary over time, which allows for reducing any impacts of outliers such as during the COVID-19 pandemic (see, e.g., Carriero *et al.*, 2024).

The link between quarterly observed and monthly latent variables is established with a set of $i = 1, \ldots, n_1$, measurement equations:

$$y^*_{1,it} = \frac{1}{3}y_{1,it} + \frac{2}{3}y_{1,it-1} + y_{1,it-2} + \frac{2}{3}y_{1,it-3} + \frac{1}{3}y_{1,it-4} + \eta_{it}, \quad \eta_{it} \sim \mathcal{N}(0, \omega_i^2), \tag{2}$$

where η_{it} is a measurement error. Equation (2) is called an intertemporal restriction for log-growth rates, which exists whenever we observe a quarterly measure (i.e., for $t = 3, 6, 9, \ldots$), see also Mariano and Murasawa (2003). We follow Chan *et al.* (2023) and introduce measurement errors, with a small variance $\omega_i^2 = 1e^{-8}$, in the intertemporal restriction, to acknowledge the approximate nature of the triangular weighting scheme for latent growth rates. A side-effect of this choice are computational advantages for larger systems of equations.

2.2. Nonlinearities in the conditional mean functions

In our modeling framework, we use Bayesian Additive Regression Trees (BART, Chipman *et al.*, 2010) to model $\boldsymbol{F}(\boldsymbol{x}_t) = (f_1(\boldsymbol{x}_t), \ldots, f_n(\boldsymbol{x}_t))'$. BART uses a sum regression trees, each acting as step-function partitioning the input space provided by x_t. Each tree has terminal nodes that provide fitted values for the output variables. Similar in spirit to random forests, BART uses many simple trees instead of one complex tree. While each tree only explains a small portion of the variance, collectively, they capture complex nonlinear relationships.

The conditional mean functions are approximated equation-by-equation:

$$f_i(\boldsymbol{x}_t) \approx \sum_{s=1}^{S} \ell_{is}(\boldsymbol{x}_t | \mathcal{T}_{is}, \boldsymbol{\mu}_{is}),$$

where S denotes the number of trees, $\mathcal{T}_{is}$ provides the tree structure and $\boldsymbol{\mu}_{is}$ contains the terminal node parameters. Due to the large number of trees, regularization is essential in BART. It can be achieved via priors on the tree-generating stochastic process, which contains the prior assumptions about $\mathcal{T}_{is}$. A prior on node depth determines the probability of a node being nonterminal, which decreases with depth. The probability of a node at depth d being nonterminal is set to $\alpha/(1+d)^{\beta}$, where $\alpha \in (0,1)$ and $\beta \in \mathbb{R}^{+}$. We follow the default values, $\alpha = 0.95$ and $\beta = 2$, as specified by Chipman *et al.* (2010), which have been shown to work well in a large number of contexts. Further, we specify a discrete uniform prior over the splitting variables, which implies that all variables are equally likely to act as determining the partitions of the input space. Lastly, the thresholds within the splitting rules are also assigned a uniform prior over the range of the relevant splitting variables. We now turn to the prior parameters of the terminal nodes. With $\#\text{TN}_{is}$ denoting the number of terminal node parameters of tree s, we choose independent Gaussian priors that are symmetric across trees for the terminal node parameters, such that $\mu_{is,l} \sim \mathcal{N}(0, v_i)$ for $l = 1, \dots, \#\text{TN}_{is}$. The prior variance $\sqrt{v_i}$ is driven in a data-driven way such that $\sqrt{v_i} = \frac{\max(\boldsymbol{y}_i)-\min(\boldsymbol{y}_i)}{2\gamma\sqrt{S}}$. This implies that most prior mass is put on the observed range of values where $\boldsymbol{y}_i = (y_{i1}, \dots, y_{iT})'$.

A recent survey of BART in a multivariate time series context is provided in Marcellino and Pfarrhofer (2024). For further details about the implementation, we refer the technically inclined reader to Pfarrhofer and Stelzer (2025), who use an identical prior setup and sampling algorithm. Given this prior setup, regularization arises primarily from two sources. First, the prior on tree depth favors shallow (i.e., more simplistic rather than complex) trees. Second, the tightness of the prior on the terminal node parameters increases with the number of trees, which implies more shrinkage on the output values. Despite these regularization measures, it is possible to obtain larger and more complex trees when required. Finally, we choose $S = 250$ for the number of trees, which strikes a balance between having too few trees and using needlessly many of them.

This setup establishes a nonlinear state space model. A more detailed description of the prior setup and estimation algorithm are provided in Appendix A. In short, we follow Huber *et al.* (2023); Marcellino and Pfarrhofer (2025) and use a linear approximation for obtaining smoothed estimates of the states. This allows a standard Gibbs sampling algorithm featuring a precision sampling step, that is, we iterate between sampling all model parameters and the latent monthly processes.

2.3. Nonlinear shock impacts and dynamic causal effects

We estimate dynamic causal effects that arise from the difference of two potential outcomes, see, e.g., Jordà and Taylor (2024). The conditional IRF is defined as:

$$\tilde{\mathrm{IRF}}(d, \boldsymbol{\Omega}_t)_{j,h} \equiv \tilde{\boldsymbol{\delta}}_{t,j,h}^{(d,d_0)} = \mathbb{E}(\boldsymbol{y}_{t+h} \mid \varepsilon_{jt} = d_0 + d, \boldsymbol{z}_t) - \mathbb{E}(\boldsymbol{y}_{t+h} \mid \varepsilon_{jt} = d_0, \boldsymbol{z}_t), \tag{3}$$

where $\boldsymbol{z}_t$ refers to the dependence on the initial conditions at t. The latter term in the equation above refers to a baseline scenario, where the jth shock takes a value of $d_0 \in \mathbb{R}$; the first term is another scenario where the jth shock takes the value $d_0 + d$. Here, $d \in \mathbb{R}$ can be set to any desired number which encodes shock sign and magnitude. In such a setup, we compare a change of magnitude d in the structural shock, relative to some baseline value d_0 of the shock. We store conditioning arguments specific to each period t in $\boldsymbol{\Omega}_t = (d_0, \boldsymbol{z}_t')'$. That is, we estimate the difference in between two expectations conditional on different values of the structural shock.[2] This is also referred to as a generalized IRF (GIRF) in the spirit of Koop *et al.* (1996). To allow for easier interpretation, we compute the scaled version $\mathrm{IRF}(d, \boldsymbol{\Omega}_t)_{j,h} \equiv \boldsymbol{\delta}_{t,j,h}^{(d,d_0)} = \tilde{\boldsymbol{\delta}}_{t,j,h}^{(d,d_0)}/d \equiv \tilde{\mathrm{IRF}}(d, \boldsymbol{\Omega}_t)_{j,h}/d$. These rescaled IRFs "neutralize" sign and magnitude dependent differences but leave asymmetries in terms of shapes or persistence in responses unchanged for straightforward (visual) comparisons. More detailed information on how to compute dynamic causal effects in our nonparametric context is provided in Appendix A and Pfarrhofer and Stelzer (2025). We provide a brief discussion of the related considerations below.

First, we assume that $\boldsymbol{F}(\boldsymbol{z}_t, \boldsymbol{\varepsilon}_t) = \boldsymbol{H}(\boldsymbol{z}_t) + \boldsymbol{G}(\boldsymbol{\varepsilon}_t)$. Analogous to Section 2.1 these functions are equation-specific: $\boldsymbol{H}(\boldsymbol{z}_t) = (h_1(\boldsymbol{z}_t), \ldots, h_n(\boldsymbol{z}_t))'$ and $\boldsymbol{G}(\boldsymbol{\varepsilon}_t) = (g_1(\boldsymbol{\varepsilon}_t), \ldots, g_n(\boldsymbol{\varepsilon}_t))'$.

[2] For a comprehensive taxonomy of different definitions of dynamic causal effects and their relationships, see Rambachan and Shephard (2021) and Gonçalves *et al.* (2024).

That is, there may be nonlinearities of the structural shocks on impact measured by the function $\boldsymbol{G}$, but these are unrelated to the lagged dependent variables.

Second, on impact of the observed shock, it is worth noting that the baseline level of the shock d_0 matters (in contrast to linear models). Intuitively, for an increase of size $d = 1$, the impact on a variable may be different depending on whether the initial value of the shock is, for example, $d_0 = 0$ or $d_0 = 1$. We randomly vary over different baseline levels of the shock to account for this notion.

Third, higher-order responses are computed by simulating the shock and baseline scenarios forward, where the required conditional expectations based on (3) are known h-by-h. Variation due to future reduced form shocks is thus addressed via a Monte Carlo approach; variation in future structural shocks is introduced with a bootstrap procedure, where we draw randomly from the observed shocks with replacement.

Forth, we can in principle compute (3) for each t, and these IRFs feature time variation which is due to different initial conditions. To average out this random variation, we use a bootstrap procedure, see also Kilian and Lütkepohl (2017, chapter 18). That is, we draw a random sample $\mathcal{R}$ of size R with replacement from $\{1, 2, \ldots, T\}$, compute the conditional IRFs, and then take an average: $\text{IRF}(d)_{j,h} = \frac{1}{R}\sum_{r\in\mathcal{R}} \text{IRF}(d, \tilde{\boldsymbol{\Omega}}^{(r)})_{j,h}$.[3] Doing so for a reasonably large number R in each sweep of our MCMC algorithm yields draws from the desired unconditional estimate, $\text{IRF}(d)^{(k)}_{j,h}$.

3. HETEROGENEOUS EFFECTS OF MONETARY POLICY

Using the econometric framework described in Section 2, we study the transmission of monetary policy in the EA through bank-based transmission channels. The sampling period ranges from January 2003 to September 2023, that is, we have $T = 249$ monthly observations, while there are 83 observations for the quarterly series. Detailed informa-

[3] In case interest centers on specific sub-periods, such as recessions vs. expansions, we use the same procedure but define admissible sets of initial conditions according to the respective classification (e.g., suppose there is a recession only in periods $5, 6, 7$, then $\mathcal{R}_{\text{recession}}$ is based on a sample from these periods exclusively; $\mathcal{R}_{\text{expansion}}$, by contrast, can only feature periods other than these).

tion on data sources and transformations for all variables are available in Appendix B, below we provide a description of the most important aspects.

The monthly data on macroeconomic and financial variables include consumer price inflation, industrial production, a stock market index, financial conditions measured by a corporate spread, and a short term interest rate. These variables are collected in $\boldsymbol{y}_{\mathrm{h},t}$. Another endogenous variable, observed on a quarterly frequency, is aggregate real GDP growth in the EA (labeled *output* below) which is featured in $\boldsymbol{y}_{1,t}$. This information set coincides roughly with recent related work, see, for instance, Jarociński and Karadi (2020).

To account for bank-based transmission of monetary policy, we supplement these "hard" data with data from the BLS. This survey collects information on bank lending conditions in the EA.[4] Questions are addressed to senior loan officers of a representative sample of EA banks and is conducted on a quarterly basis. We follow Ciccarelli *et al.* (2013) in using the information from BLS questions that describe changes in credit standards for and demand of loans to firms and households (for both credit for house purchase, consumer credit and other lending), as well as factors that affected these changes in lending conditions over the past three months. This survey-based information helps us to trace different credit-related channels of monetary policy transmission. In particular, we use information from the question on changes in credit standards to define the broad *credit* channel that captures bank's general willingness to lend in response to monetary policy (beyond interest rates). Furthermore, we use banks' answers to the questions about the factors that contributed to changes in credit standards in order to characterize the two subchannels of the broad credit channel. When banks' answers report that the economic outlook and risk were determining factors in easing or tightening their credit standards, we relate this to the *borrower balance sheet channel*, or bank's lending attitude based on perceived risks or collateral value. Similarly, the bank *lending* channel is constructed on the basis of factors contributing to changes in credit standards related to banks' capital, financing, liquidity or competition. These reflect the constraints

[4] See data.ecb.europa.eu/methodology/bank-lending-survey-bls for a detailed description of the BLS.

on banks' own balance sheets in response to monetary policy that could affect lending.[5] Lastly, we us banks' answers about changes in loan demand to characteriue and control for credit *demand*.

BLS data that is publicly available and reported as net percentage changes, which is the difference between the share of banks reporting that credit standards applied to loan approval (or demand for loans) have been tightened (increased) and the share of banks reporting that they have been eased (decreased). Each of the channels we mentioned above is reflected in distinct groups of variables, which are typically strongly correlated. To obtain aggregate measures, we thus extract common factors using the first principle component for each block of variables associated with the respective channel. The resulting four (quarterly) time series of common factors that measure these channels are featured in $\boldsymbol{y}_{1,t}$. The original interpretation of the BLS data remains in the factors: An increase/decrease indicates a tightening/easing of credit standards or in the case of credit demand, an increase of the factor indicates an increase in demand for loans by firms and households.

Perhaps the most crucial variable is the monetary policy shock ε_t. As discussed in our econometric framework in Section 2, we abstract from identification of the shock in a narrow sense (within our model); rather, the shock enters the model as observed and exogenous data. This simplifies estimation and computing the dynamic causal effects. The data for the monetary policy shock is sourced from the webpage of Marek Jarocinski, who provides posterior median estimates (`MP_median`) of the shocks obtained from running the model proposed in Jarociński and Karadi (2020). Their approach uses high-frequency surprises around monetary policy announcement dates combined with sign restrictions in a Bayesian VAR. Their procedure orthogonalizes the pure monetary policy shock from contaminating information effects. A chart of this time series is provided in Figure 5 of Section 3.3.

[5] Appendix B provides further details on which BLS questions are used in constructing the three bank-based transmission channels.

3.1. Which types of asymmetries are there on impact?

Figures 1 and 2 shows the nonlinear impact effect on observed variables $i = 1, \ldots, n$, as a function of the shock over an evenly spaced grid of values $\varepsilon_l \in [\min(\{\varepsilon_t\}_{t=1}^T), \max(\{\varepsilon_t\}_{t=1}^T)]$, for $l = 1, \ldots, \mathbb{L}$, i.e., the impact response $\delta_{i0}^{(\varepsilon_l,0)} = g_i(\varepsilon_l) - g_i(0)$, see also Appendix A. These charts are partial dependence plots, which are common in the machine learning literature to visually inspect effect sizes. They can also be used to gauge the shape of the functional relationship between the shock and the respective observed variable on impact.

The nonparametric BART-based estimates are in solid black with grey shaded 50/68 percent posterior credible sets. Additional lines are approximations estimated with OLS for specific functional forms of nonlinearities, which serve as visual references.[6]

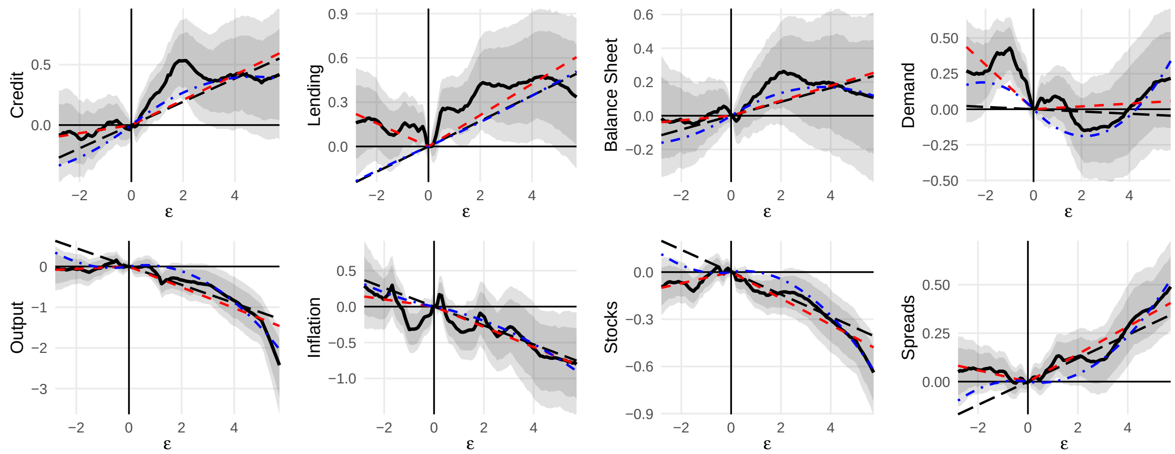

Figure 1: Nonlinear impact effects on selected observed variables as a function of the shock ε. Positive values of ε indicate a tightening, negative values an easing of monetary policy. Nonparametric estimate in solid black with grey shaded 50/68 percent posterior credible sets. Additional lines are approximations for specific functional forms: linear (dashed black line), sign nonlinearity (red dashed line), size nonlinearity (blue dot-dashed line).

The upper row in figure 1 show impact responses of the bank lending channels as well as credit demand as measured by the BLS. Both the credit and balance sheet

[6] Linear (dashed black line) shows fitted values of regressing $\delta_{i0}^{(\varepsilon_l,0)} = \beta_{i1} \cdot \varepsilon_l + e_l$; sign nonlinearity (red dashed line) with $\delta_{i0}^{(\varepsilon_l,0)} = \beta_{i1} \cdot \varepsilon_l + \beta_{i2} \cdot |\varepsilon_l| + e_l$; and size nonlinearity (blue dot-dashed line) with $\delta_{i0}^{(\varepsilon_l,0)} = \beta_{i1} \cdot \varepsilon_l + \beta_{i2} \cdot \varepsilon_l \cdot |\varepsilon_l| + e_l$.

channel display similar responses to a monetary policy shock. While monetary policy easing has a negligible effect, regardless of the size of the shock, the response to monetary policy tightening is much more significant. In particular, the impact responses increase for larger shock sizes up to $\epsilon = 2$. Beyond that, the response levels out, regardless of the size of the shock, which suggests a threshold effect. Therefore, both size and sign nonlinearities are present in the impact responses of the credit and balance sheet channel.

The bank lending channel shows a somewhat different impact response pattern. It indicates a small tightening even in response to an easing shock, although these impact responses are not significant, and show no significant size dependencies. Positive shocks, however, result in relatively large tightening impulses in the bank lending channel, that increase up to $\epsilon = 4$. Impact responses to credit demand indicates that demand increases in response to a monetary policy easing, with a steep increase in relative effect up to $\epsilon = -2$. Beyond that, the effects level out and become insignificant. Monetary policy tightening, however, does not result in significant responses in credit demand on impact.

The lower row in figure 1 contains the impact responses of macroeconomic variables to a monetary policy shock. Impact responses of output to monetary policy easing are virtually flat. Responses to a monetary tightening are very similar to those implied in a linear model, but for shock sizes for $\epsilon > 4$, they indicate disproportionately large negative impact responses (i.e., a size asymmetry, but only for contractionary shocks). Impact responses of stocks and spreads show a similar pattern of sign and size asymmetries. In contrast, inflation does not exhibit the same response pattern. Monetary policy easing only results in positive impact reactions when the shock is sufficiently large ($\epsilon < -1.5$). A surprise monetary policy tightening results in a similar type of "price puzzle" after small shocks up to about 1sd, and only more substantial tightening results in decreased inflation.

Impact responses of short term and long term interest rates show mostly muted responses for both monetary policy easing and tightening. Part of the explanation for this finding is that short term interest rates were close to the the ELB in much of our sample, and there is thus only a limited amount of variation to exploit for estimation.

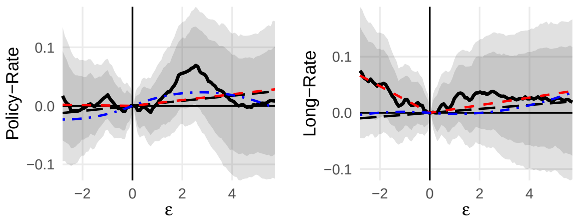

Figure 2: Nonlinear impact effects on interest rates as a function of the shock ε. Positive values of ε indicate a tightening, negative values an easing of monetary policy. Nonparametric estimate in solid black with grey shaded 50/68 percent posterior credible sets. Additional lines are approximations for specific functional forms: linear (dashed black line), sign nonlinearity (red dashed line), size nonlinearity (blue dot-dashed line).

Impact responses of the short term interest rates, however, remain quite close to the effects in a linear model (which are also small); see, for instance, Jarociński and Karadi (2020). Long term interest rates, on the other hand, show some sign asymmetries. While impact responses stay insignificant overall, a higher posterior mass indicates that long term interest rates tend to response with an increase to monetary policy easing.

It is worth noting that despite interest rates displaying a muted response to monetary policy shocks, the credit, bank lending and balance sheet channel as well as macroeconomic and financial variables react to monetary policy, both on impact and at higher horizons (as discussed in the following sections). Combined with the fact that the factors we extract from the BLS to measure bank based transmission is based more broadly on credit standards, rather than narrowly on interest rates, this suggests that a strong response in interest rates is not always necessary to elicit a monetary tightening or easing.

Compared with the parametric functional forms (colored lines), it is worth noting that these approximations in many cases offer a poor fit. This suggests that more flexible shapes (as estimated with our BART implementation) are required to adequately characterize the nonlinearities on impact.

3.2. An aggregate view of asymmetric monetary policy effects

Before discussing nonlinearities in the dynamic responses to monetary policy, we note that a linear version of our framework produces responses in line with theory and previous empirical findings (e.g., such as Jarociński and Karadi, 2020); see also Appendix B for additional details and a discussion. Next, we turn to our detailed analysis of different potential nonlinearities in dynamic responses to monetary policy. It reveals that a linear specification such as the one mentioned above conceals several asymmetries, specifically when it comes to shocks of different signs.

Credit variables

Figure 3 contains responses of bank based transmission channels to monetary policy shocks of different signs and magnitudes. We see that the credit, bank lending and the balance sheet channel react with a tightening to a contractionary monetary policy shock. In panel 3b, responses of the credit and bank lending channel are significant for over 12 months for a 1sd shock and up to 24 months for larger, 3sd shocks. Responses in the balance sheet channel to a 1sd shock are less significant, but when considering a larger shocks, responses remain significantly different from zero for the whole IRF horizon. As suggested by theory, credit demand reacts negatively to a contractionary shock, with stronger and more significant responses to a larger than to a smaller shock. Interestingly, responses of credit demand display more nonlinearities with regards to the size of the shock after a expansionary monetary policy shock. While responses to a 3sd shock are disproportionally small, responses to a 1sd shock are much more pronounced. Generally, expansionary shocks elicit muted responses in bank lending, which is particularly true for larger shocks.

Turning to the possibility of asymmetric responses with regard to a the sign of the shock, we see a repetition of the pattern we saw in responses on impact. Bank lending responses to expansionary monetary policy shocks are subdued and mostly insignificant, with the exception of the response of credit demand to a 1sd expansionary shock. In contrast, responses to contractionary shocks are mostly significant and according to theory. Interestingly, the asymmetries in bank lending responses become more distinct with increasing shock size.

Macro variables

Figure 4 contains impulse responses of selected macroeconomic variables to a monetary policy shock. Panel 4a compares the scaled impulse responses of output, inflation, stocks and spreads to a 1sd and a 3sd monetary policy shock. With the exception of inflation, responses to neither expansive or contractive monetary policy shocks of different sizes display any particularly notable nonlinearities. Responses of inflation to contractionary shocks are significant for both a 1sd and a 3sd shock, but the scaled response to a 1sd shock is larger than a 3sd shock. This indicates, that inflation's response (in terms of the posterior median) to larger contractionary shocks is disproportionally smaller, which is a pattern we can also observe for stock market prices and, to a smaller degree, spreads. In contrast, in responses of inflation to a 3sd expansionary monetary policy shock, more posterior mass lies on lower values than in responses to a 1sd shock. While these responses are not statistically different from each other, this could point to the fact that more forceful monetary policy easing is required to impact inflation. A more distinct pattern of sign asymmetries in responses becomes apparent when turning to panel 4b. While contractionary policy shocks result in textbook responses that are mostly significant, responses to an expansionary shock are rather muted. Financial variables display particularly strong asymmetries with respect to the sign of the shock.

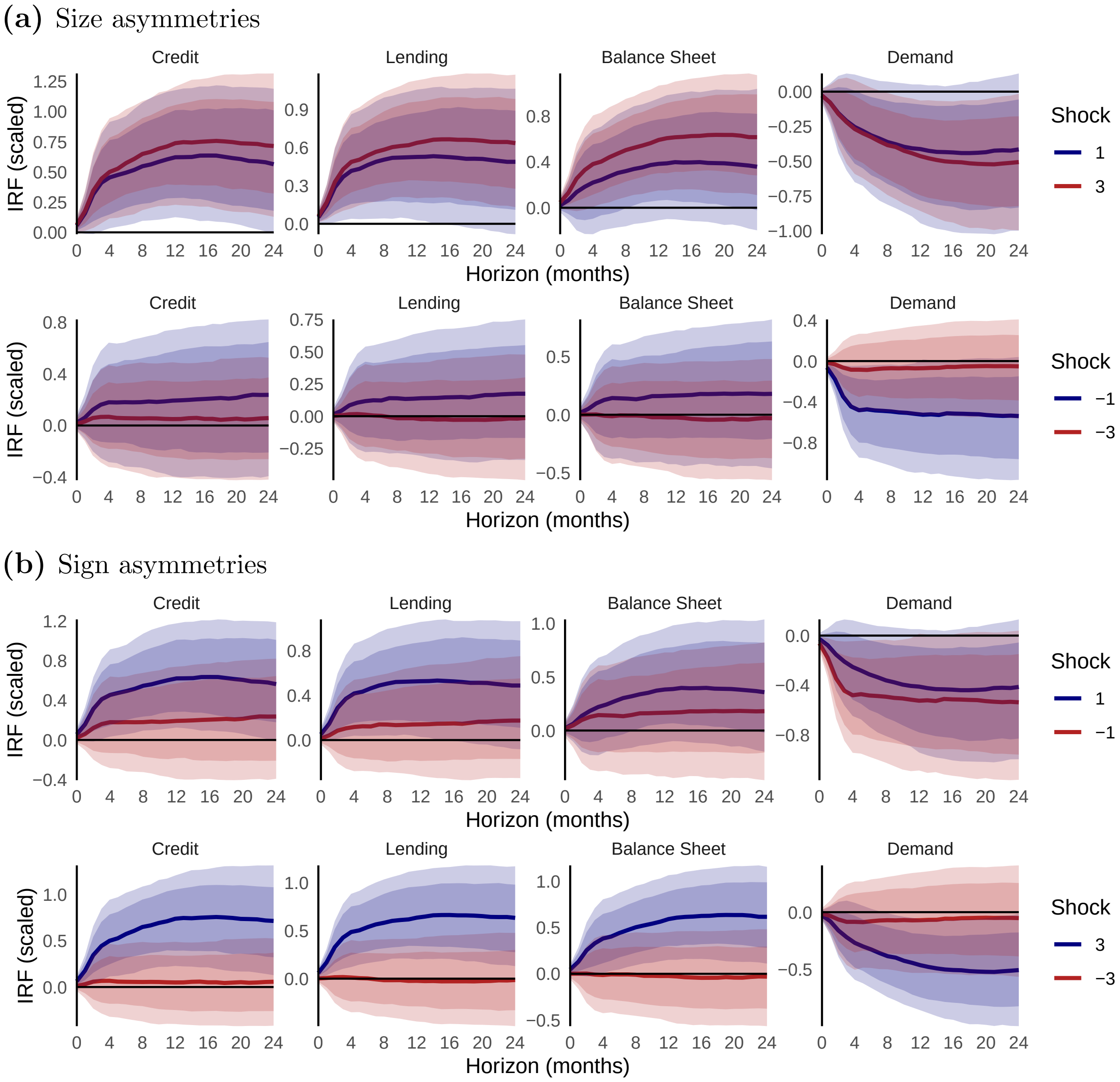

Figure 3: Impulse response functions for credit variables to a monetary policy shock, comparing asymmetries due to size and sign of the shocks.

Notes: Posterior median alongside 50 and 68 percent credible sets. To allow for straightforward visual comparisons, all IRFs are scaled/normalized to a one standard deviation contractionary shock as described in Section 2.3.

(a) Size asymmetries

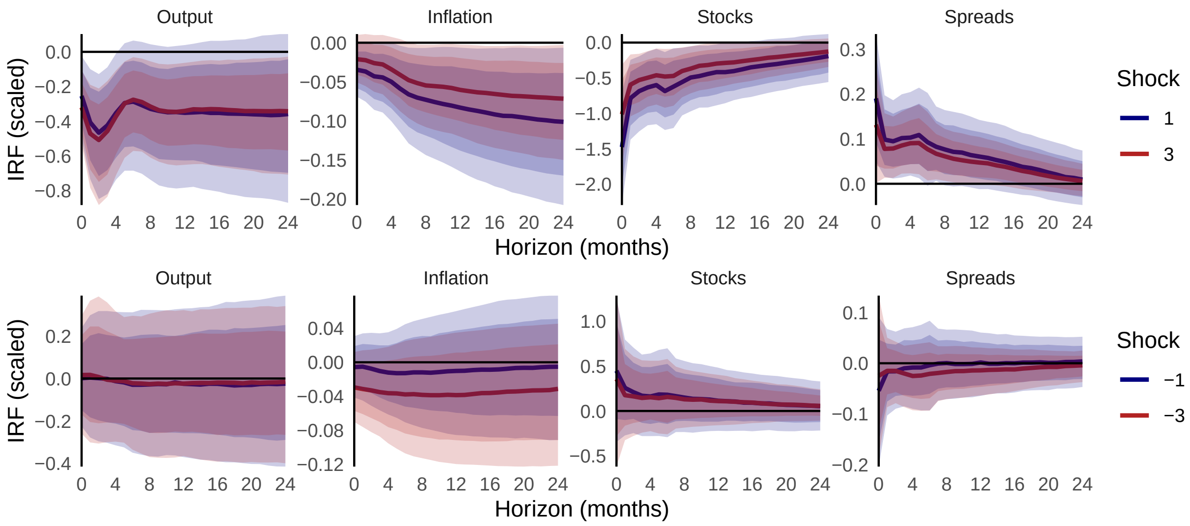

(b) Sign asymmetries

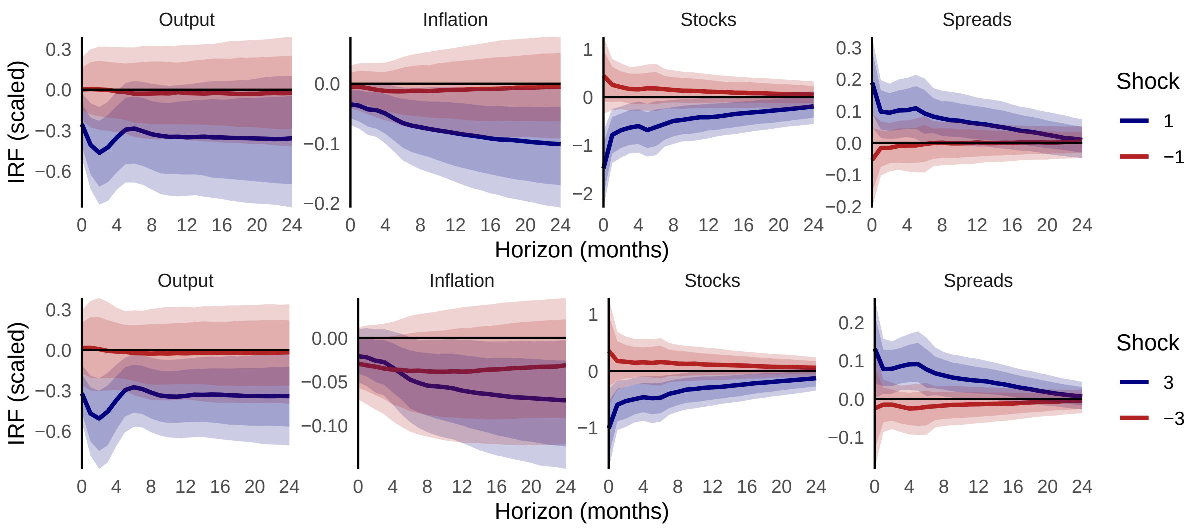

Figure 4: Impulse response functions for selected macroeconomic and financial variables to a monetary policy shock, comparing asymmetries due to size and sign of the shocks.

Notes: Posterior median alongside 50 and 68 percent credible sets. To allow for straightforward visual comparisons, all IRFs are scaled/normalized to a one standard deviation contractionary shock as described in Section 2.3.

3.3. State-dependent effects of monetary policy

In order to further understand the origins of these asymmetries, we examine the potential of state-dependent nonlinearities. As explained in section 2.3, the following IRFs are estimated with full sample information, but computed with distinct initial conditions for the respective sub-samples. Building on our insights from our previous results, in the following, we mostly focus on sign asymmetries. For reference, plots showing size asymmetries are included in figures B.2 and B.3 in the appendix.

The different sub-samples we consider are (1) expansions versus recessions, as defined by the Euro Area Business Cycle Dating Committee; and (2) the ELB, defined for periods where the euro short-term rate was below 25 basis points, similar to Carriero *et al.* (2025) for US data. While EA short term rates in part were substantially below zero, we follow this convention because any related decisions may be constrained, and nonlinearities may already arise, even before zero or negative interest occur. Figure 5

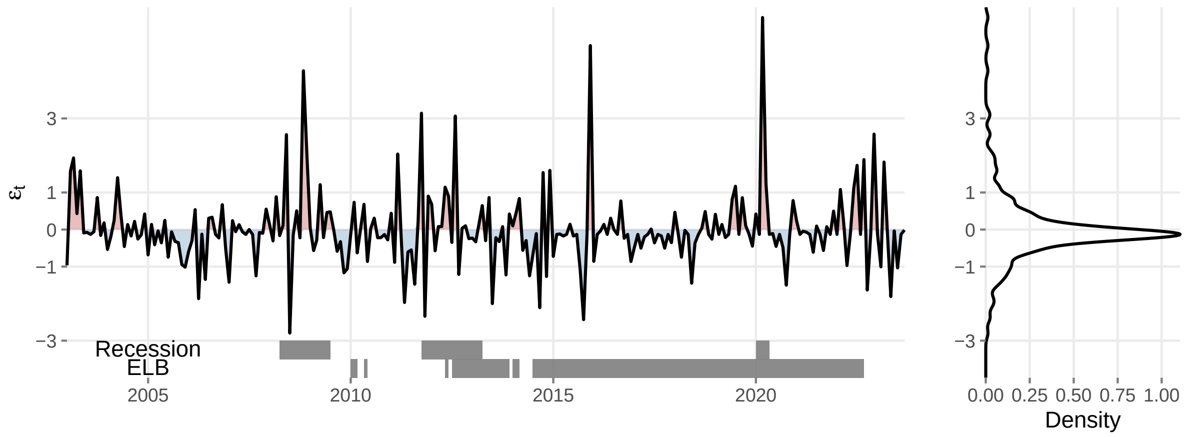

Figure 5: Monetary policy shock time series and smoothed kernel density estimate. Blue and red indicate expansionary and contractionary shocks, respectively. The grey bars at the bottom indicate the recession and ELB sub-samples.

shows the monetary policy shock time series and a smoothed kernel density estimate. The grey bars at the bottom indicate the recession and ELB sub-samples. A few comments are in order. First, we want to point out that based on the way monetary policy shocks are constructed by Jarociński and Karadi (2020), an expansionary/contractionary monetary policy shock is not synonymous with an interest rate cut/hike. Second, both positive and negative shocks can occur during an expansion/a recession as well as at the ELB and away from the ELB. This implies that our results below are not driven by the fact that recessions tend to coincide with monetary policy easing, or that conventional monetary policy faced challenges to accommodate further easing at the ELB.

State-dependence: Expansions versus recessions

We start our discussion of possible state-dependencies by comparing responses during expansions to those during recessions. In order to accommodate another dimension of our results besides sign and size of the shock, we choose to show our IRFs in the form of boxplots for selected horizons. This not only allows for a more clearly arranged overview of both expansionary and contractionary shocks during both expansions and recessions. Illustrating IRFs in boxplot-form also makes it possible to see more easily when responses are overlapping or, in contrast, are statistically different from each other while still allowing to follow the form of the IRFs over different horizons. For consistency and better comparison, all responses are again scaled to a 1sd contractionary monetary policy shock.

Figure 6 shows the responses of bank lending and selected macroeconomic and financial variables to both a 1sd contractionary (light blue/red) and expansionary shock (dark blue/red) in panel 6a, and 3sd shocks in panel 6b in an expansion (depicted in two shades of blue) and a recession (depicted in shades of red).

Interestingly, responses to a 1sd expansionary shock are mostly muted, no matter whether they occur during a recession or an expansion. This holds true for almost all variables, with the exception of credit demand. Contractionary monetary policy shows more effectiveness, but again, this is true for both expansions and recessions. Even though the median response to a contractionary shock during expansions tends to be a bit more pronounced than during recessions (especially for the bank lending channels and inflation), responses are not significantly different from each other.

For the most part, the same dynamic patterns appear in panel 6b. A loosening of monetary policy results in mostly insignificant responses during both expansions and recessions, even though we can observe more posterior mass below zero in the response of inflation to a larger expansionary shock. Contractionary shocks, on the other hand, result in significant responses for most variables and IRF horizons. For most variables, credible sets become smaller for larger shocks, resulting in less overlapping of the four possible combinations of size, sign and state of the economy. However, there is still no clear distinction between responses, hinting that state-dependencies play less of a role than overall sign of the monetary policy shock.

Implications of the effective lower bound

We next turn to monetary policy effects during the ELB, which constitutes a significant part of our data sample. Figure 7 shows the IRF responses in boxplot form to both a 1sd contractionary (light blue/red) and expansionary shock (dark blue/red) in panel 7a, and 3sd shocks in panel 7b during times at the ELB (depicted in two shades of blue) versus times away from the ELB (depicted in shades of red).[7]

Insights from the ELB are in line with those comparing recessions and expansions. Expansionary monetary policy remains mostly ineffective, with the exception of 1sd monetary policy shocks, which always result in significant responses of credit demand. In contrast, responses to contractionary shocks are both significantly different from zero and from expansionary shocks. Sign asymmetries remain the dominant factor, with no differences between responses during the ELB and away from the ELB.

[7] The presence of the ELB has resulted in an increased importance of other monetary policy instruments, such as quantitative easing and forward guidance. Whilst the analysis of potential nonlinearities in the transmission of these instruments is of particular interest during the period at the ELB, we deliberately decide against including such an analysis due to the very rich set of results and insights offered by our examination of conventional monetary policy. The investigation of unconventional monetary policy is left for future research (relatedly, see, e.g., Hauzenberger *et al.*, 2021, for insights on time-variation in the effects of quantitative easing and forward guidance due to different levels of uncertainty in the economy).

(a) 1sd shock

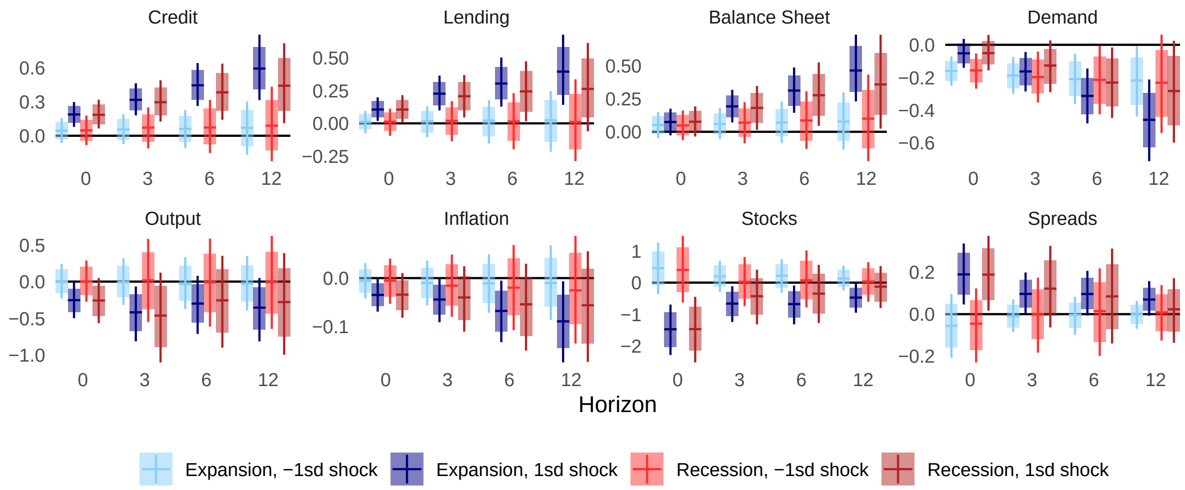

(b) 3sd shock

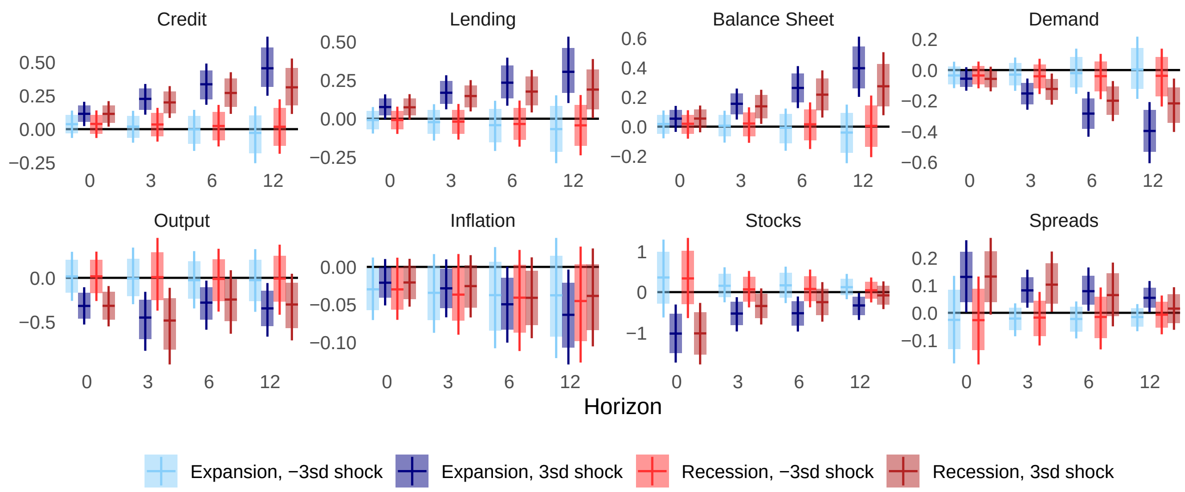

Figure 6: Sign asymmetries for state dependent (scaled) IRFs in expansions and recessions for a subset of credit, macroeconomic and financial variables across selected horizons.

Notes: Posterior median alongside 50 and 68 percent credible sets. To allow for straightforward visual comparisons, all IRFs are scaled/normalized to a one standard deviation contractionary shock as described in Section 2.3. Expansions and recessions are defined according to the Euro Area Business Cycle Dating Committee.

(a) 1sd shock

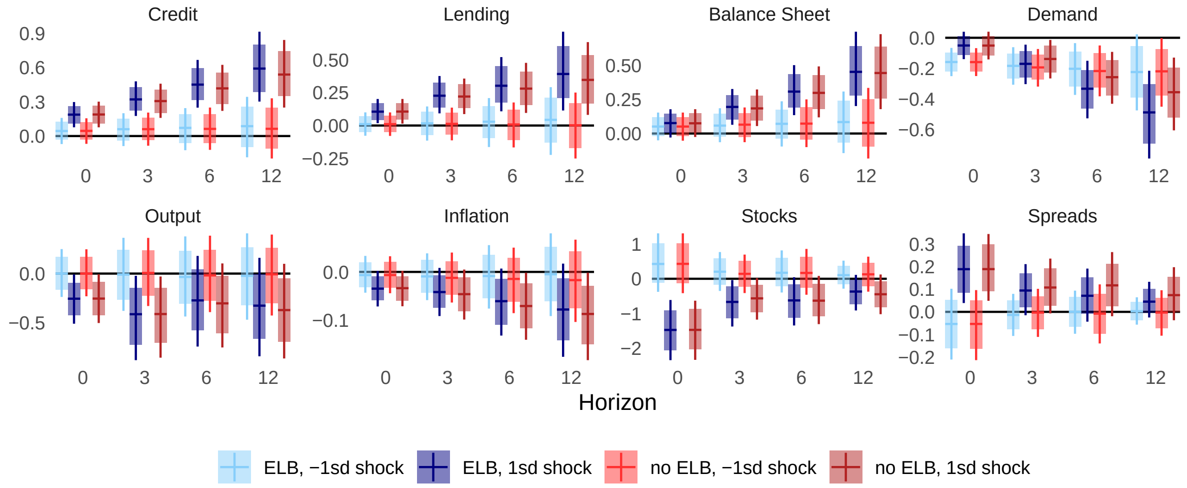

(b) 3sd shock

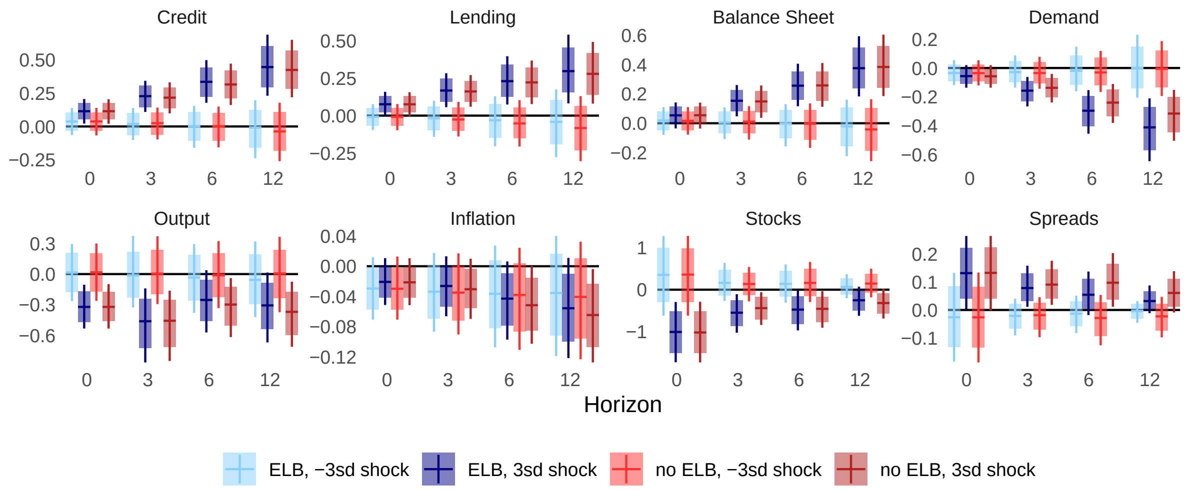

Figure 7: Sign asymmetries for state dependent (scaled) IRFs at the effective lower bound (ELB) for a subset of credit, macroeconomic and financial variables across selected horizons.

Notes: Posterior median alongside 50 and 68 percent credible sets. To allow for straightforward visual comparisons, all IRFs are scaled/normalized to a one standard deviation contractionary shock as described in Section 2.3. Periods where the policy rate was below 25 basis points were categorized as "ELB."

4. CONCLUSIONS AND FUTURE RESEARCH

This paper uses a nonlinear mixed-frequency BART model to analyze how monetary policy shocks affect macroeconomic and financial variables in the EA, with a focus on bank lending channels. Our findings suggest that monetary policy transmission via the credit channel and its sub-channels in the EA is asymmetric. Contractionary monetary policy shocks have stronger and more consistent effects than expansionary ones. In fact, our analysis suggests that expansionary monetary policy is largely ineffective, which is true both during recessions and at the ELB. Credit demand remains an exception, which is modestly affected by expansionary monetary policy shocks.

All bank lending channels considered, the credit, bank lending and balance sheet channel, respond significantly to contractionary shocks. These effects are persistent and are somewhat amplified for larger shocks. Macroeconomic and financial variables such as output, inflation, stocks or spreads show textbook responses to a monetary tightening, but muted or nonlinear reactions to easing. While we do find evidence for the presence of some nonlinearities with respect to the size of a monetary policy shock, sign asymmetries dominate our overall results. The direction of the shock tends to matter even more than the state of the business cycle or the presence of the ELB. Generally, state-dependence of monetary policy effects is limited, suggesting that asymmetries are not primarily driven by the economic state, but rather the sign of a monetary policy shock. This finding is similar to those in the literature on estimating state-dependent fiscal multipliers (Barnichon *et al.*, 2022), where previously identified state-dependence can in part be explained by the distribution of shocks arising from distinct identification schemes, and their distribution across time.

Our nonlinear modeling reveals dynamics that would be missed by a linear model, which highlights the importance of flexible, data-driven approaches in monetary policy analysis. Overall our results are in line with previous research on asymmetric effects of monetary policy, which often find contractionary monetary policy to be more effective than expansionary (Matthes *et al.*, 2015; Tenreyro and Thwaites, 2016; Angrist *et al.*, 2018). Beyond reaffirming the presence of sign asymmetries in bank-based monetary policy transmission in the EA, our detailed analysis of the different origins of nonlinearities provides further insight. These suggest that state dependency may play a smaller role than previously thought. Central banks should therefore be cautious in expecting symmetric effects from monetary policy easing and tightening. Tightening is more potent, while easing may require complementary tools to be equally as effective. Especially with regards to a price stability mandate, easing might also require larger monetary policy easing to achieve the same proportionate effect on inflation as a mirrored monetary tightening would have.

For future research, using alternative monetary policy shock series, e.g., those of Altavilla *et al.* (2025), might offer robustness. Furthermore, in conjunction with the framework of Pfarrhofer and Stelzer (2025), our model lends itself to counterfactual exercises, such as an analysis of the 2022–2023 tightening cycle. Investigating how the effects of monetary policy on the real economy would have differed if the credit channel had remained neutral would not only help us to deepen our understanding of the credit channel in an unprecedented tightening cycle, but also to evaluate the relative importance of this transmission channel.

REFERENCES

Altavilla C, Gürkaynak RS, Laeven L, and Kind T (2025), "Monetary transmission with frequent policy events," .

Angrist JD, Jordà Ò, and Kuersteiner GM (2018), "Semiparametric estimates of monetary policy effects: string theory revisited," *Journal of Business & Economic Statistics* **36**(3), 371–387.

Barigozzi M, Conti AM, and Luciani M (2014), "Do euro area countries respond asymmetrically to the common monetary policy?" *Oxford bulletin of economics and statistics* **76**(5), 693–714.

Barnichon R, Debortoli D, and Matthes C (2022), "Understanding the size of the government spending multiplier: It's in the sign," *The Review of Economic Studies* **89**(1), 87–117.

Barnichon R, and Matthes C (2018), "Functional approximation of impulse responses," *Journal of Monetary Economics* **99**, 41–55.

Bernanke BS, and Gertler M (1995), "Inside the black box: the credit channel of monetary policy transmission," *Journal of Economic perspectives* **9**(4), 27–48.

Boivin J, Giannoni MP, and Mojon B (2008), "How has the euro changed the monetary transmission?" Technical report, National Bureau of Economic Research.

Caravello T, and Martinez-Bruera P (2024), "Disentangling Sign and Size Nonlinearities," *SSRN* **4704050**.

Carriero A, Clark TE, Marcellino M, and Mertens E (2024), "Addressing COVID-19 outliers in BVARs with stochastic volatility," *Review of Economics and Statistics* 1–15.

——— (2025), "Forecasting with shadow rate VARs," *Quantitative Economics* **16**(3), 795–822.

Chan JC (2023), "Comparing stochastic volatility specifications for large Bayesian VARs," *Journal of Econometrics* **235**(2), 1419–1446.

Chan JC, and Jeliazkov I (2009), "Efficient simulation and integrated likelihood estimation in state space models," *International Journal of Mathematical Modelling and Numerical Optimisation* **1**(1-2), 101–120.

Chan JC, Poon A, and Zhu D (2023), "High-dimensional conditionally Gaussian state space models with missing data," *Journal of Econometrics* **236**(1), 105468.

Chipman HA, George EI, and McCulloch RE (2010), "BART: Bayesian additive regression trees," *The Annals of Applied Statistics* **4**(1), 266–298.

Ciccarelli M, Maddaloni A, and Peydró JL (2013), "Heterogeneous transmission mechanism: monetary policy and financial fragility in the eurozone," *Economic Policy* **28**(75), 459–512.

Clark T, Huber F, and Koop G (2025), "A Nonparametric Approach to Augmenting a Bayesian VAR with Nonlinear Factors," *arXiv* **2508.13972**.

Clark TE, Huber F, Koop G, Marcellino M, and Pfarrhofer M (2023), "Tail forecasting with multivariate Bayesian additive regression trees," *International Economic Review* **64**(3), 979–1022.

Conti AM, Neri S, and Notarpietro A (2024), "Credit strikes back: the macroeconomic impact of the 2022-23 ECB monetary tightening and the role of lending rates," *Bank of Italy Occasional Paper* (884).

Corsetti G, Duarte JB, and Mann S (2021), "One Money, Many Markets," *Journal of the European Economic Association* **20**(1), 513–548.

Crawford L, Wood KC, Zhou X, and Mukherjee S (2018), "Bayesian approximate kernel regression with variable selection," *Journal of the American Statistical Association* **113**(524), 1710–1721.

Dahlhaus T (2017), "Conventional monetary policy transmission during financial crises: An empirical analysis," *Journal of Applied Econometrics* **32**(2), 401–421.

Esser J, Maia M, Parnell AC, Bosmans J, van Dongen H, Klausch T, and Murphy K (2024), "Seemingly unrelated Bayesian additive regression trees for cost-effectiveness analyses in healthcare," *arXiv* **2404.02228**.

Favero C, Giavazzi F, and Flabbi L (1999), "The transmission mechanism of monetary policy in Europe: evidence from banks' balance sheets," .

Foroni C, and Marcellino M (2014), "Mixed-frequency structural models: Identification, estimation, and policy analysis," *Journal of Applied Econometrics* **29**(7), 1118–1144.

Gargiulo V, Matthes C, and Petrova K (2025), "Monetary policy across inflation regimes," *European Economic Review* 105109.

Ghysels E (2016), "Macroeconomics and the reality of mixed frequency data," *Journal of Econometrics* **193**(2), 294–314.

Gonçalves S, Herrera AM, Kilian L, and Pesavento E (2024), "State-dependent local projections," *Journal of Econometrics* **244**(2), 105702.

Hauzenberger N, Pfarrhofer M, and Stelzer A (2021), "On the effectiveness of the European Central Bank's conventional and unconventional policies under uncertainty," *Journal of Economic Behavior & Organization* **191**, 822–845.

Huber F, Koop G, Onorante L, Pfarrhofer M, and Schreiner J (2023), "Nowcasting in a pandemic using non-parametric mixed frequency VARs," *Journal of Econometrics*

232(1), 52–69.

Ish-Horowicz J, Udwin D, Flaxman S, Filippi S, and Crawford L (2019), "Interpreting deep neural networks through variable importance," *arXiv* **1901.09839**.

Jarociński M, and Karadi P (2020), "Deconstructing monetary policy surprises–The role of information shocks," *American Economic Journal: Macroeconomics* **12**(2), 1–43.

Jordà Ò, and Taylor AM (2024), "Local Projections," *Journal of Economic Literature* **forthcoming**.

Kilian L, and Lütkepohl H (2017), *Structural vector autoregressive analysis*, Cambridge University Press.

Koop G, Pesaran MH, and Potter SM (1996), "Impulse response analysis in nonlinear multivariate models," *Journal of Econometrics* **74**(1), 119–147.

Lane PR (2023), "Speech by Philip R. Lane, Cambridge, Massachusetts, 12 July 2023," https://www.ecb.europa.eu/press/key/date/2023/html/ecb.sp230712~d950906f00.en.html, accessed: 02-04-2025.

Lenza M, and Primiceri GE (2022), "How to estimate a vector autoregression after March 2020," *Journal of Applied Econometrics* **37**(4), 688–699.

Marcellino M, and Pfarrhofer M (2024), "Bayesian Nonparametric Methods for Macroeconomic Forecasting," in MP Clements, and AB Galvao (eds.) "Handbook of Macroeconomic Forecasting," Edward Elgar Publishing Ltd.

——— (2025), "Nonparametric mixed frequency monitoring macro-at-risk," *Economics Letters* 112498.

Mariano RS, and Murasawa Y (2003), "A new coincident index of business cycles based on monthly and quarterly series," *Journal of Applied Econometrics* **18**(4), 427–443.

Matthes C, Barnichon R, *et al.* (2015), "Measuring the non-linear effects of monetary policy," in "2015 Meeting Papers," 49, Society for Economic Dynamics.

Peek J, Rosengren ES, *et al.* (1995), "Bank lending and the transmission of monetary policy," in "Conference series-federal reserve bank of Boston," volume 39, 47–68, Federal Reserve Bank of Boston.

Pfarrhofer M, and Stelzer A (2025), "Scenario analysis with multivariate Bayesian machine learning models," *arXiv* **2502.08440**.

Primiceri GE (2005), "Time varying structural vector autoregressions and monetary policy," *The Review of Economic Studies* **72**(3), 821–852.

Rambachan A, and Shephard N (2021), "When do common time series estimands have nonparametric causal meaning?" *Mimeo* .

Romer CD, and Romer DH (2004), "A new measure of monetary shocks: Derivation and implications," *American Economic Review* **94**(4), 1055–1084.

Schorfheide F, and Song D (2015), "Real-time forecasting with a mixed-frequency VAR," *Journal of Business & Economic Statistics* **33**(3), 366–380.

Sims CA, and Zha T (2006), "Were there regime switches in US monetary policy?" *American Economic Review* **96**(1), 54–81.

Tenreyro S, and Thwaites G (2016), "Pushing on a string: US monetary policy is less powerful in recessions," *American Economic Journal: Macroeconomics* **8**(4), 43–74.

Weise CL (1999), "The asymmetric effects of monetary policy: A nonlinear vector autoregression approach," *Journal of Money, Credit and Banking* 85–108.

Online Appendix: Are there asymmetries in euro area monetary policy?

A. TECHNICAL APPENDIX

A.1. Variants of impulse response functions

The IRF on impact can generally be computed as $\boldsymbol{\delta}_{t,0}^{(d,d_0)} = \boldsymbol{F}(\boldsymbol{z}_t, \boldsymbol{\varepsilon}_t^{(d+d_0)}) - \boldsymbol{F}(\boldsymbol{z}_t, \boldsymbol{\varepsilon}_t^{(d_0)})$. We assume that $\boldsymbol{F}(\boldsymbol{z}_t, \boldsymbol{\varepsilon}_t) = \boldsymbol{H}(\boldsymbol{z}_t) + \boldsymbol{G}(\boldsymbol{\varepsilon}_t)$. In this case, the IRF on impact is given by $\boldsymbol{\delta}_{t,0}^{(d,d_0)} = \boldsymbol{G}(\boldsymbol{\varepsilon}_t^{(d+d_0)}) - \boldsymbol{G}(\boldsymbol{\varepsilon}_t^{(d_0)})$. Additional discussions on functional forms that are commonly assumed for $\boldsymbol{G}(\bullet)$, are provided below.

For higher-order responses, Pfarrhofer and Stelzer (2025) discuss sequential Monte Carlo methods to explore the posterior of the expectation of the respective distributions horizon-by-horizon. These are needed due to the nonlinearities, to compute the IRF in Equation (3). We use their particle Gibbs with ancestor sampling (PGAS) algorithm, extended with a bootstrap-type approach to account for the contemporaneous presence of the observed structural shocks.

Following Kilian and Lütkepohl (2017, chapter 18), similar to $\boldsymbol{\Omega}_t$ from earlier, define $\tilde{\boldsymbol{\Omega}}_t = (d_0, \boldsymbol{\varepsilon}'_{t:t+h}, \boldsymbol{z}'_t)'$ and denote the kth draw from the posterior of the IRF as $\boldsymbol{\delta}_{t,j,h}^{(d,d_0;k)} = \text{IRF}(d, \tilde{\boldsymbol{\Omega}}_t)_{j,h}^{(k)}$, i.e., as a function of the shock size d and the "history" $\tilde{\boldsymbol{\Omega}}_t$ at horizon h for structural shock j, and a path of the structural shocks. The unconditional IRF is:

$$\text{IRF}(d)_{j,h}^{(k)} = \int \text{IRF}(d, \tilde{\boldsymbol{\Omega}}^{(k,r)})_{j,h} \mathrm{d}\tilde{\boldsymbol{\Omega}}^{(k,r)} \approx \frac{1}{R}\sum_{r=1}^{R} \text{IRF}(d, \tilde{\boldsymbol{\Omega}}^{(k,r)})_{j,h},$$

where $\tilde{\boldsymbol{\Omega}}^{(k,r)}$ is a randomly selected history for $r = 1, \ldots, R$. Choosing a reasonably large number of random histories R and repeating this procedure in each draw of our sampling algorithm marginalizes over the parameters of our model, see also Pfarrhofer and Stelzer (2025) for related discussions. We thus obtain draws from the desired posterior of $\text{IRF}(d)_{j,h}$.

A.2. Functional forms for sign and size asymmetries

Other options to measure asymmetries, which are more easily interpretable in return (i.e., in terms of distinguishing between sign and size asymmetries), can be implemented by assuming a specific symmetric functional form across equations $i = 1, \ldots, n$. In this case we may treat the shocks across $j = 1, \ldots, m$, fully independently, so for simplicity, consider a single shock ε_t:

$$g_i(\varepsilon_t) = \beta_{i1}\varepsilon_t + \beta_{i2}\tilde{g}(\varepsilon_t), \quad \boldsymbol{G}(\varepsilon_t) = \boldsymbol{\beta}_1\varepsilon_t + \boldsymbol{\beta}_2\tilde{g}(\varepsilon_t).$$

This is the approach discussed in, e.g., Caravello and Martinez-Bruera (2024). Assuming a linear contemporaneous response is achieved by setting $\boldsymbol{\beta}_2 = \mathbf{0}_n$. The IRF at $h = 0$ is then simply given by $\boldsymbol{\delta}_{t,0}^{(d,d_0)} = d \cdot \boldsymbol{\beta}_1$. This implies that these responses are constant over time and proportional on impact, and nonlinearities only arise for higher-order responses when iterated forward through $\boldsymbol{F}(\bullet)$. When assuming functional forms to measure asymmetries on impact, one may choose to investigate distinct types of nonlinearities (due to either sign or size) when specifying $\tilde{g}$. For sign nonlinearities, we pick $\tilde{g}(\varepsilon_t) = |\varepsilon_t|$. For size nonlinearities, we use $\tilde{g}(\varepsilon_t) = \varepsilon_t \cdot |\varepsilon_t|$. The IRF on impact in either case is $\boldsymbol{\delta}_{t,0}^{(d,d_0)} = d \cdot \boldsymbol{\beta}_1 + (\tilde{g}(d_0 + d) - \tilde{g}(d_0)) \cdot \boldsymbol{\beta}_2$, which may be simplified further to $\boldsymbol{\delta}_{t,0}^{(d,0)} = d \cdot \boldsymbol{\beta}_1 + \tilde{g}(d) \cdot \boldsymbol{\beta}_2$ when $d_0 = 0$.

A.3. Bayesian inference

The covariance matrix $\boldsymbol{\Sigma}_t = o_t^2\boldsymbol{\Sigma}$ has a constant part $\boldsymbol{\Sigma}$ scaled by o_t^2, which relates to common stochastic volatility VARs (see, e.g., Chan, 2023). This time-varying scalar may capture huge-variance shocks and outliers such as during the pandemic of the early 2020s. Our nonparametric framework for the conditional mean functions is in principle robust to outliers (compared with linear VAR models) and even captures specific forms of heteroskedasticity without an explicit treatment in error terms (see Clark *et al.*, 2023, for a discussion). To provide further robustness and reflect the recent literature (see, e.g., Lenza and Primiceri, 2022), we introduce an additional safeguard against such observations. Specifically, we use a variant of Carriero *et al.* (2024), and assume that:

$$o_t = \begin{cases} 1 & \text{with probability} \quad 1-\mathfrak{p} \\ \mathcal{U}(2,6) & \text{with probability} \quad \mathfrak{p}, \end{cases}$$

where $\mathcal{U}(\bullet)$ is a discrete uniform distribution with support between 2 and 6 and $\mathfrak{p}$ is the probability associated with observing an outlier. The constant part of the covariance matrix $\boldsymbol{\Sigma}$ is assigned a hierarchical inverse Wishart prior, as suggested by Esser *et al.* (2024).

Approximate sampling of the latent states

Define $\boldsymbol{y} = (\boldsymbol{y}_1', \ldots, \boldsymbol{y}_T')'$, $\boldsymbol{F} = (\boldsymbol{F}(\boldsymbol{x}_1)', \ldots, \boldsymbol{F}(\boldsymbol{x}_T)')'$ and $\boldsymbol{\epsilon} = (\boldsymbol{\epsilon}_1', \ldots, \boldsymbol{\epsilon}_T')'$, $\boldsymbol{X} = (\boldsymbol{x}_1, \ldots, \boldsymbol{x}_T)'$ and $\boldsymbol{O} = \text{diag}(o_1^2, \ldots, o_T^2)$. Then we may rewrite Eq. (1) in stacked notation as:

$$\boldsymbol{y} = \boldsymbol{F} + \boldsymbol{\epsilon}, \quad \boldsymbol{\epsilon} \sim \mathcal{N}(\mathbf{0}_{Tn}, \boldsymbol{O} \otimes \boldsymbol{\Sigma}).$$

We define $\boldsymbol{X}^*$ to be the Moore-Penrose inverse of $\boldsymbol{X}$, and rely on a linear approximation of our model $\boldsymbol{A} = \boldsymbol{X}^* \boldsymbol{F}$. This approach is inspired by Ish-Horowicz *et al.* (2019); Crawford *et al.* (2018), and has been employed in a multivariate mixed-frequency BART context in Huber *et al.* (2023). We obtain $\boldsymbol{y} = \boldsymbol{X}\boldsymbol{A} + \boldsymbol{\epsilon}$, where $\boldsymbol{A} = (\boldsymbol{A}_1, \ldots, \boldsymbol{A}_P)'$ are the linearized dynamic coefficients, partitioned such that $\boldsymbol{A}_p$ is associated with the pth lag in $\boldsymbol{x}_t$. See also Marcellino and Pfarrhofer (2025) for a more technical discussion.

Having linearly approximated the dynamic coefficients, we can use standard tools for linear Gaussian state space models to obtain the approximate posterior of the latent states. Here, we rely on the precision sampler of Chan and Jeliazkov (2009) for estimation which renders estimation of large systems feasible.

Sampling algorithm

Our algorithm is based on Gibbs sampling and iterates between drawing the latent states (i.e., the unobserved high frequency processes associated with the low frequency variables) and all model parameters. We initialize the design matrices, and then proceed as follows:

1. Sample the model parameters conditional on the observed data and latent states:
   - Update the regression trees equation-by-equation, see also Esser *et al.* (2024) and Pfarrhofer and Stelzer (2025) for the equation-specific moments of the respective posteriors. This includes the splitting variables, thresholds and terminal node parameters.
   - Conditional on the data and the trees, we update the constant part of the covariance matrix from its inverse Wishart posterior; conditional on the draw for $\mathbf{\Sigma}$ the hierarchical parameters of this prior can be sampled. The outlier adjustment parameters o_t can be sampled t-by-t from their discrete posterior.
2. Sample the latent states conditional on all model parameters:
   - Using the approximation, we obtain a set of linearized dynamic coefficients that we can use in conjunction with a precision sampler to efficiently update all latent variables.

These are the main steps of the MCMC algorithm. We run this algorithm for 12,000 times, discarding the initial 3,000 draws as burn-in and retain each 3rd of the remaining draws. These draws can be used to compute the dynamic causal effects in the form of the IRFs described in Section 2.3 and above (in this Appendix).

B. EMPIRICAL APPENDIX

B.1. Data

Table B.1: Data, transformations and source.

Variable	Description	FQ / $h(x)$ / Details	Source
Inflation (`hicp`)	Harmonized Index of Consumer Prices	M / 3 / s.a.	FRED
Stock market (`es50`)	Euro Stoxx 50 Equity Index	M / 2	ECB SDW
Production (`indprod`)	Industrial production	M / 3 / w.a., s.a.	ECB SDW
Spreads (`spreads`)	ICE BofA Euro High Yield Index OAS	M / 1 / %	FRED
Interest rate (`DE_1y`)	1-year Bund bond yield	M / 1 / %	Macrobond
Output (`gdp`)	Real gross domestic product (GDP)	Q / 3 / s.a.	ECB SDW

Notes: Data from the FRED database of the Federal Reserve Bank of St. Louis is available for download at fred.stlouisfed.org. Abbreviations: frequency (FQ), option-adjusted spread (OAS), working day adjusted (w.a.), seasonally adjusted (s.a.); numbers for $h(x_t)$ indicate transformations: (1) levels x_t, (2) log-levels $100 \cdot \log(x_t)$, (3) log-differences $100 \cdot \log(x_t/x_{t-1})$.

Table B.2: BLS data and corresponding transmission channel.

BLS Variable Description	**Channel**
Change in credit standards for ...	
... loans to enterprises ... loans to HHs for house purchase ... consumer credit and other lending to HHs	(Broad) Credit
Change in demand for...	
... loans to enterprises ... loans to HHs for house purchase ... consumer credit and other lending to HHs	Demand
Factors contributing to changes in credit standards for loans to enterprises	
Costs related to bank's capital position Bank's ability to access market financing Bank's liquidity position Competition from other banks Competition from non-banks Competition from market financing	Bank lending
General economic situation and outlook Industry or firm-specific situation and outlook Risk related to the collateral demanded	Borrower balance sheet
Factors contributing to changes in credit standards for loans for house purchase	
Costs related to bank's capital position Cost of funds and balance sheet constraints (until 2021Q4) Bank's ability to access market financing Bank's liquidity position Competition from other banks Competition from non-banks	Bank lending
General economic situation and outlook Housing market prospects, incl. expected house price developments Borrower's creditworthiness	Borrower balance sheet
Factors contributing to changes in credit standards for consumer credit and other lending to households	
Costs related to bank's capital position Cost of funds and balance sheet constraints (until 2021Q4) Bank's ability to access market financing Bank's liquidity position Competition from other banks Competition from non-banks	Bank lending
General economic situation and outlook Creditworthiness of consumers	Borrower balance sheet

Notes: All series are available on a quarterly basis and are summarized as weighted net percentage (tightened minus eased or reverse) or net demand (increased minus decreased) over the past three months.

B.2. Additional results

Figure B.1 displays the responses of macroeconomic and financial variables to a 1sd contractionary monetary policy shock in a linear specification of our modeling setup. Note that for variables that enter our model in differences, the reported results are cumulative responses over the horizons.

The three variables capturing the credit and sub-channel, credit, lending and balance sheet channel, react with a tightening. The response of the balance sheet channel is statistically significant for one quarter, while the response of the credit channel remains significant for about two quarters. The response of the lending channel displays significant posterior mass above zero, but is never significantly different from zero. Credit demand is reduced significantly and persistently in response to a monetary policy tightening. Consequently, real variables such as output, production and prices (which enter our model in differences) display significant and persistent responses to a contractionary monetary policy shock. The response of the policy rate is significantly positive for about two months after impact, while long term rates are lowered persistently after a contractionary monetary policy shock, albeit this response is not statistically significantly different from zero. Stock valuations decrease significantly for about two quarters, while the response of financial conditions (measured by spreads) indicates a tightening, which is, however, not significant.

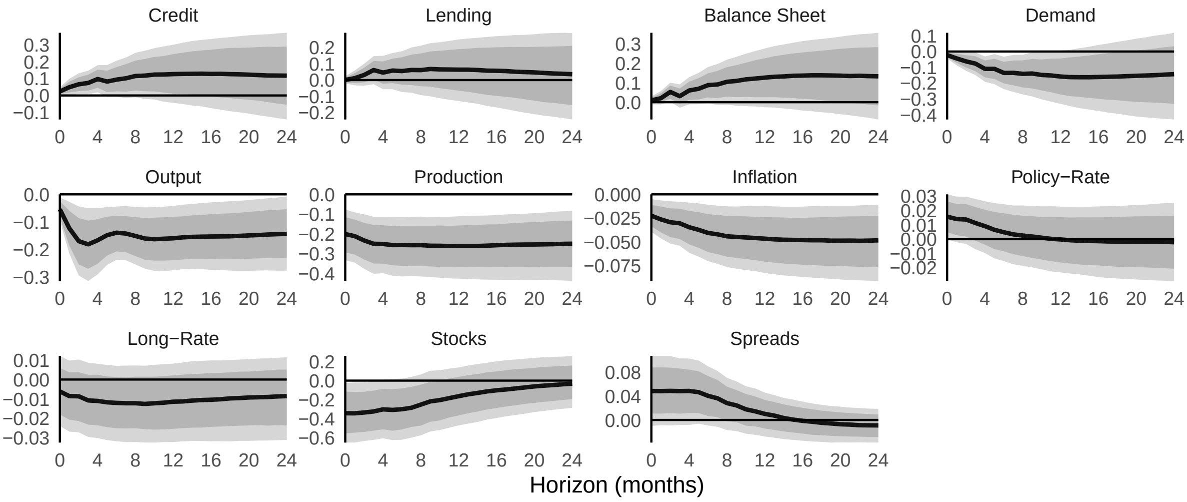

Figure B.1: Impulse response functions for macroeconomic and financial variables of our model to a 1sd contractionary monetary policy shock in a linear VAR model.

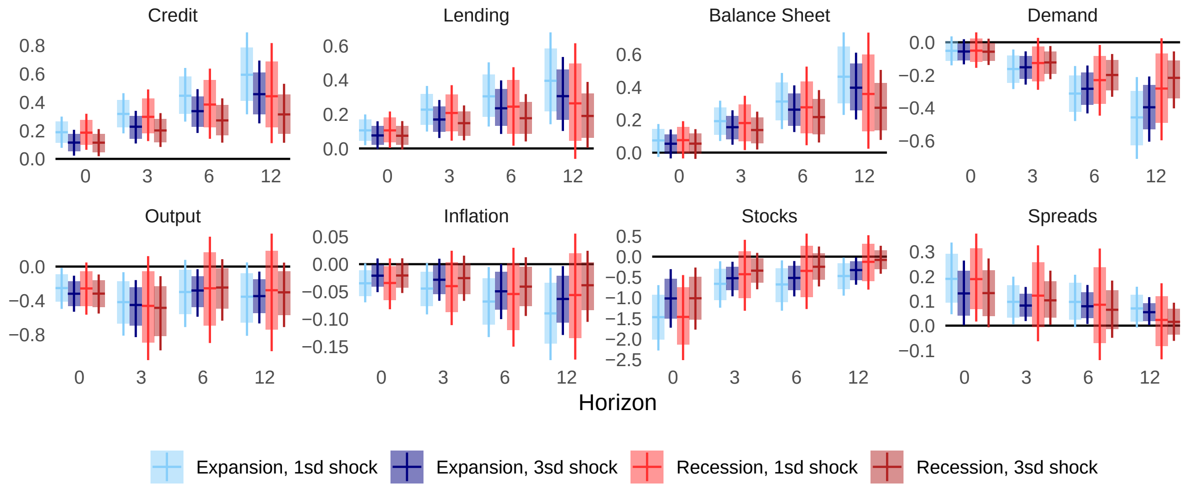

Figure B.2: Size asymmetries for state dependent (scaled) IRFs in expansions and recessions for a subset of credit, macroeconomic and financial variables across selected horizons.

Notes: Posterior median alongside 50 and 68 percent credible sets. To allow for straightforward visual comparisons, all IRFs are scaled/normalized to a one standard deviation contractionary shock as described in Section 2.3. Expansions and recessions are defined according to the Euro Area Business Cycle Dating Committee.

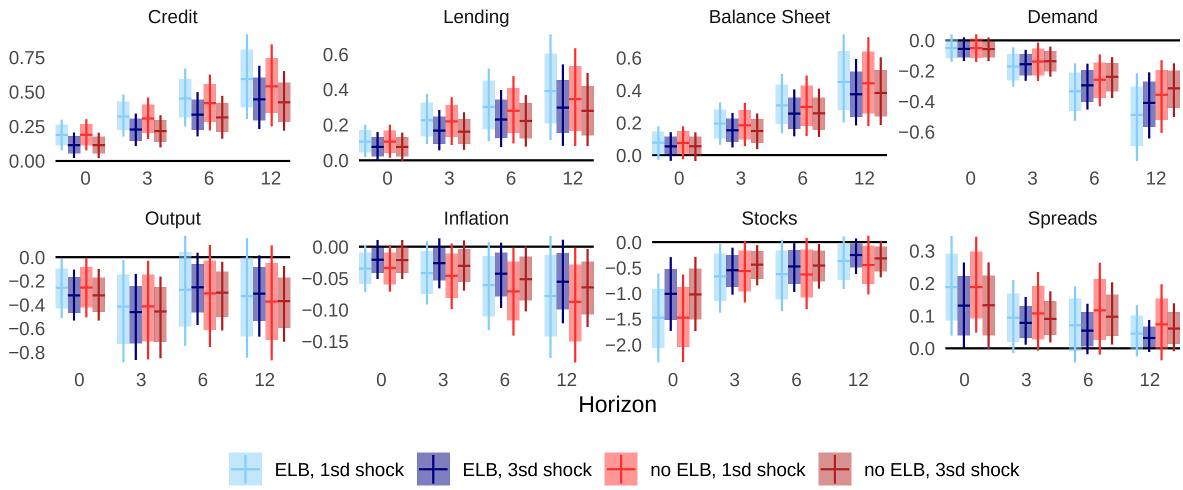

Figure B.3: Size asymmetries for state dependent (scaled) IRFs at the effective lower bound (ELB) for a subset of credit, macroeconomic and financial variables across selected horizons.

Notes: Posterior median alongside 50 and 68 percent credible sets. To allow for straightforward visual comparisons, all IRFs are scaled/normalized to a one standard deviation contractionary shock as described in Section 2.3. Periods where the policy rate was below 25 basis points were categorized as "ELB."

The Working Paper series of the Oesterreichische Nationalbank is designed to disseminate and to provide a platform for discussion of either work of the staff of the OeNB economists or outside contributors on topics which are of special interest to the OeNB. To ensure the high quality of their content, the contributions are subjected to an international refereeing process. The opinions are strictly those of the authors and do in no way commit the OeNB.

The Working Papers are also available on our website (http://www.oenb.at) and they are indexed in RePEc (http://repec.org/).

Publisher and editor Oesterreichische Nationalbank
Otto-Wagner-Platz 3, 1090 Vienna, Austria
PO Box 61, 1011 Vienna, Austria
www.oenb.at
oenb.info@oenb.at
Phone (+43-1) 40420-6666

Editor Martin Summer

Cover Design Information Management and Services Division

DVR 0031577

ISSN 2310-533X (Online)